Reaching quantum accuracy in predicting adsorption properties for ethane/ethene in ZIF-8 at the low pressure regime

Siddharth Ravichandran,[†] Mahsa Najafi,[‡] Ruben Goeminne,[†] Joeri F.M. Denayer,[‡] Veronique Van Speybroeck,[*,†] and Louis Vanduyfhuys[*,†]

[†]*Center for Molecular Modeling (CMM), Ghent University, Technologiepark 46, 9052, Zwijnaarde, Belgium*

[‡]*Department of Chemical Engineering, Vrije Universiteit Brussel, Pleinlaan 2, 1050, Brussels, Belgium*

E-mail: veronique.vanspeybroeck@ugent.be; louis.vanduyfhuys@ugent.be

Abstract

Nanoporous materials in the form of Metal-Organic Frameworks (MOFs) such as zeolitic imidazolate framework-8 (ZIF-8) are promising membrane materials for separation of hydrocarbon mixtures. To compute the adsorption isotherms in such adsorbents, grand canonical Monte Carlo (GCMC) simulations have proven very useful. The quality of these isotherms depend on the accuracy of adsorbate-adsorbent interactions which are mostly described using force fields owing to their low computational cost. However, force field predictions of adsorption uptake often show discrepancies from experiments at low pressures, providing the need for methods that are more accurate. Hence, in this work, we propose and validate two novel methodologies for the ZIF-8/ethane and ethene systems; a benchmarking methodology to evaluate the performance of any given force field in describing adsorption in the low-pressure regime

and a refinement procedure to rescale the parameters of a force field to better describe the host-guest interactions and provide for simulation isotherms with close agreement to experimental isotherms. Both methodologies were developed based on a reference Henry coefficient, computed with the PBE-MBD functional using the importance sampling technique. The force field rankings predicted by the benchmarking methodology involves the comparison of force field derived Henry coefficients with the reference Henry coefficients and ranking the force fields based on the disparities between these Henry coefficients. The ranking from this methodology matches the rankings made based on uptake disparities by comparing force field derived simulation isotherms to experimental isotherms in the low-pressure regime. The force field rescaling methodology was proven to refine even the worst performing force field in UFF/TraPPE. The uptake disparities of UFF/TraPPE improved from 197% and 194% to 11% and 21% for ethane and ethene respectively. The proposed methodology is applicable to predict adsorption across nanoporous materials and allows for rescaled force fields to reach quantum accuracy without the need for experimental input.

1. Introduction

In recent years, there has been an urgent need for industries to adopt sustainable and energy-efficient separation and purification technologies to achieve net-zero carbon emissions. Separation of olefins from paraffins is a key industrial application where there is a significant potential for gains to be made in terms of energy efficiency[1]. Among the alternative technologies proposed for this application, adsorptive membrane separation has emerged as a front-runner due to its superior energy and separation efficiency, low cost, scalability and sustainability[2–6]. Since the separation process relies on preferential adsorption of one olefin/paraffin component over another in a mixture, the choice of the adsorbent plays an important role in determining the permeance and selectivity of the separation. The lack of suitable adsorbent material had been a key reason for membrane technology to be held back until very recently. The emergence of porous materials in the form of Metal-Organic Frameworks (MOFs) have significantly broadened the possibilities for membrane based adsorptive separation applications. MOFs, in general, possess inherent advantages over other porous materials by having a large structural diversity, modifiable functionality, large surface area and porosity[7–10]. Zeolitic imidazolate framework-8 (ZIF-8) isostructures, i.e. ZIFs with a sodalite topology, have additional desirable advantages given by framework flexibility and tunable properties[11], particularly for gas separation of light olefins/paraffins. ZIF-8 adsorbs olefin/paraffins with weak interactions and thus the energy required to regenerate the adsorbent through desorption is significantly reduced as compared to other MOFs[12]. Secondly, ZIF-8 preferentially adsorbs the paraffin over the olefin and this results in the purifying process of the more valuable olefin to be cost effective and less resource intensive. Since the cracked gas mixtures in industry contain a much larger quantity of olefin over the paraffin, a paraffin-selective adsorbent material ensures that a smaller quantity of adsorbent is sufficient for the purification process[13].

Even if the adsorption process itself is kinetically driven such as for the analysis of C2/C3 separation in ZIF-8, i.e. based on difference in diffusion, we would still need to compute

equilibrium adsorption uptake to fully simulate the difference in permeability. Developing adsorption isotherms to represent equilibrium adsorption uptake is the standard method of choice. Computational modeling offers the possibility to rapidly analyse and compare various MOF/hydrocarbon guest molecular systems by computing adsorption isotherms through grand canonical Monte Carlo (GCMC) simulations[14]. This approach offers the possibility to obtain physically meaningful information about the preferred adsorption sites and the energetics of the adsorption process. The adsorption isotherms critically depend on both host-guest and guest-guest interactions, where the host refers to the MOF framework and the guest refers to the hydrocarbon adsorbate molecule. However, as GCMC simulations require a large number of energy evaluations, force fields (FFs) have been most commonly employed in literature[13,15–17]for their low computational cost. The pertinent question concerns the accuracy of the FF, given the fact that there exists a wide variety of FFs in literature. They may either be FFs that are generic and applicable to a broad range of systems or system specific FFs.

The work of Li et al.[12] compares the predicted propane/propene uptakes in the ZIF-8 framework simulated by various literature FFs. A wide range of generic and system specific FFs that describe the ZIF-8 framework were investigated. The guest molecule, however, was described only with the TraPPE-United Atom (TraPPE)[18] FF. The results from this work illustrate that, although the qualitative predictions of the trend in propane/propene uptake is correctly predicted by all the investigated FFs, there exists large variations in terms of quantitative predictions of simulation isotherms among the different FFs.

Their work, however, compares the FF isotherms with the experimental results over a broad pressure range between 0-4 bar which includes the saturation uptake region of the isotherm. At higher loadings, the influence of guest-guest interactions increases as seen in Figure 1. The TraPPE FF, which was specifically developed to describe the bulk properties of adsorbate gases, is known to be highly accurate in capturing the guest-guest interactions[19]. Consequently, the TraPPE FF based GCMC adsorption isotherms has been shown to capture

the adsorption isotherm well in the medium to high loading regimes for different MOFs[20–22]. A good agreement of the FF isotherms with experimental isotherms at higher pressures can thus be attributed mostly to the TraPPE FF describing the adsorbate molecules and less so to the FF describing the host framework[23]. On the other hand, the agreement between the FF and experimental isotherms is generally worse in the low pressure regime[19,23] as illustrated in Figure 1. This is attributed to the poor FF descriptions of the host-guest

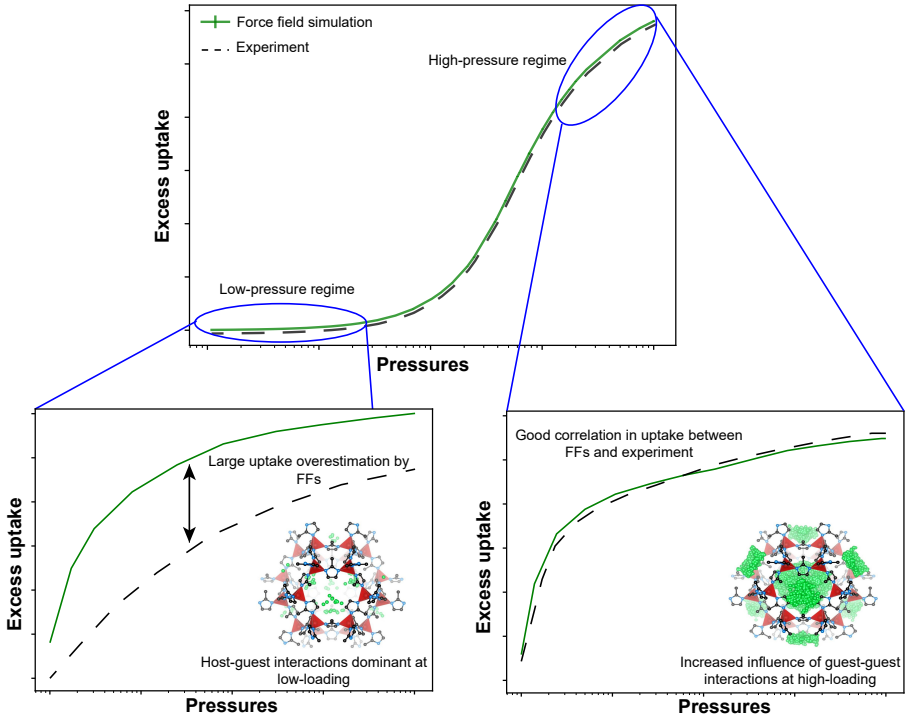

Figure 1: Schematic representation of a full adsorption isotherm illustrating the disparities in excess uptake between experimental and simulated force field isotherms; insets represent the low pressure regime and high-pressure regime of the isotherm with illustrations of the ZIF-8-adsorbate complex at different loadings; black and blue balls represent C and N atoms, red tetrahedrons represent ZnN_4 units of ZIF-8, H atoms are omitted for clarity, green balls represent adsorbate molecules.

interactions, which are predominant in the low pressure regime[23]. For porous materials such as MOFs, at low pressures, an adsorbate will preferentially adsorb in a smaller pore where there are a larger number of MOF–adsorbate interactions[24]. Further, strong confinement in porous structures, like in smaller pores, causes condensation to predominantly occur at lower pressures[25]. A focus on the low pressure regime would also provide a clearer comparison

between the different FFs that describe the host frameworks.

To address the shortcomings of predictions of low pressure adsorption properties by FFs, Fairen-Jimenez et al.[26], Pérez-Pellitero et al.[27] and Zhang et al.[28] have rescaled the FF parameters of the generic UFF force field to match available experimental results for methane[26,27] and for N_2[28]. Fairen-Jimenez et al. and Zhang et al. have uniformly reduced the ϵ_i Lennard Jones (LJ) parameter of the UFF FF describing the ZIF-8 atoms while Pérez-Pellitero et al. have reduced both ϵ_i and σ_i LJ parameters to match the experimental isotherm results. All three works claim excellent correlation with the experimental results in the low pressure regime. Fairen-Jimenez et al.[26] claim that the Henry coefficients, isosteric heats of adsorption and uptake at loadings below 30 molecules per unit cell show excellent agreement with experimental results.

However, when experimental results are not readily available like when considering new adsorbent materials, this approach will not be useful. This observation forms the motivation to develop a systematic methodology that can capture the host-guest interactions accurately without relying on experimental results. From our experience with the currently available force fields in literature, it still remains challenging to develop a force field that can accurately predict the adsorption isotherm in low-pressure regimes without requiring fitting to experimental data.

Although there have been several studies involving FF based GCMC simulations in the field of gas adsorptions in MOFs, a quantitative comparison of experimental and literature FF isotherms is unavailable. A qualitative comparison of full adsorption isotherms can often hide the large uptake overestimations by the simulated isotherms in the low pressure regime as observed in Figure 1. A numerical metric that quantifies the difference in uptake between the simulated FF isotherms and the experimental isotherms would thus be a useful tool in analysing the agreement of FFs with the experiments.

To generate adsorption isotherms or compute low pressure adsorption properties such as Henry coefficients and isosteric heats of adsorption at infinitely low loading, approximately

10^6 of Widom insertion (WI) simulations are required. This makes it too computationally expensive to describe the potential energy surface (PES) with *ab initio*[29] methods. However, an approach that is based on *ab initio* principles increases the accuracy, compared to FFs, of the description of the host-guest interactions. There have been previous attempts to investigate low pressure adsorption properties using *ab initio* calculations for various MOFs across CO_2, N_2 and CH_4[30–34]. The approaches are limited to systems with distinct adsorption sites, allowing these sites to be treated at the *ab initio* level. There are, however, other approaches that are generally applicable which have been recently introduced. Goeminne et.al.[35] proposed a procedure based on a trained machine learning potential (MLP) with a limited set of DFT intermolecular energies to generate adsorption isotherms at *ab initio* level of accuracy for ZIF-8/CO_2 and Mg-MOF-74/CO_2. Vandebrande et al.[29] have proposed a generally applicable importance sampling methodology that samples the *ab initio* PES at a fraction of the number of energy evaluations required for a traditional WI simulation to predict adsorption enthalpies and Henry coefficients. This methodology involves the selection of a limited set of configurations from a previous FF based WI simulation. As these configurations are selected with a weight equal to a Boltzmann factor of the interactions energy, they are termed as "important samples". *Ab initio* calculations are subsequently performed on this configuration set to correct the FF estimate of Henry coefficients and adsorption enthalpies, derived from the previous WI simulation. This methodology has been proven thus far to be applicable across different Covalent-Organic Frameworks (COFs) such as CO_2 and N_2 in COF-1 and COF-5[36] and MOFs such as CO_2 and methane in Mg-MOF-74 and UiO-66[29].

In this work, we aim to address two issues highlighted above concerning the computational modeling of adsorption isotherms in the low pressure regime, i.e. (1) the need for an adequate metric to assess the description of the host-guest interactions by a FF and (2) a generic methodology to rescale a given FF and elevate its predictions towards quantum accuracy. To this end, we first develop a numerical metric to compare simulated and experimental

isotherms as well as Henry coefficients. We then apply this metric to analyse the agreement of GCMC simulated isotherms using various FFs from literature with experimental isotherms for the ZIF-8/ethane and ZIF-8/ethene systems at the low pressure regime, i.e. between 0.001 to 1 bar. Furthermore, we use the Henry coefficient based metric to develop two novel methodologies; one to benchmark literature FFs at the low pressure regime and a second to rescale FFs without experimental input. Both methodologies are developed based on quantum accurate reference Henry coefficients which are determined with the importance sampling technique[29]. Finally, in order to highlight the computational efficiency of the proposed methodology we will also explicitly indicate the accuracy of predictions of the rescaled FF. The transferability of the methodology was investigated by applying it to other guest molecules, i.e propane and propene and to higher pressure regimes, i.e 0.1 to 8.1 bar. Experiments were performed at a temperature of 303K in the pressure range of 0.001 to 1 bar to obtain isotherms and Henry coefficients for the ZIF-8/ethane and ethene and ZIF-8/propane and propene systems. The various terminologies that were abbreviated in this work have been tabulated in Table S1 of Supporting Information with their respective definitions.

2. Methods

The ZIF-8 framework consists of Zn metals that are tetrahedrally coordinated by four N atoms of 2-methylimidazolate linkers and has a cubic sodalite topology. It consists of three-membered (3MR), four-membered (4MR) and six-membered ring windows (6MR) which are displayed in Figure 2. The largest interconnected six membered ring window (6MR) has an accessible diameter and pore width of 3.4 Å and 11.6 Å respectively[37–39]. ZIF-8 contains 276 atoms in each unit cell and crystallizes in a cubic space group $I\bar{4}3M$ with a lattice constant of 16.992Å[40,41]. The crystal structure of ZIF-8, which was determined experimentally, was taken from literature[37].

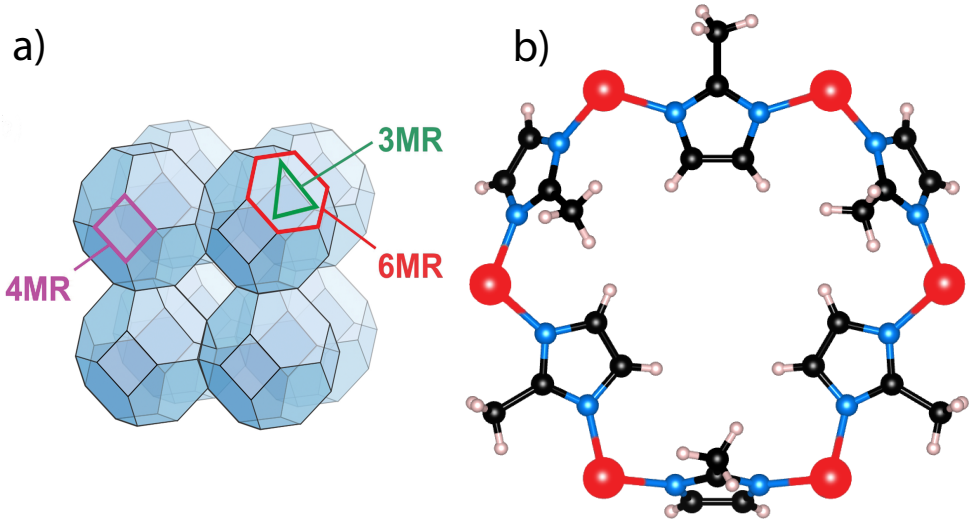

Figure 2: (a) Topological representation of the ZIF-8 framework and the different cages present in the framework. (b) Molecular representation of the largest cage of ZIF-8 (6MR); black and blue balls represent C and N atoms, red and beige balls represents Zn and H atoms respectively.

2.1 Force fields

In this work, we only consider the non-bonding contributions in literature FFs since they are applied in GCMC or Widom insertion simulations performed using a rigid framework as is common in literature[16,42–44]. Non-bonding interactions consist of van der Waals (vdW) and electrostatic interactions.

With regards to the vdW interactions, the ZIF-8 framework has been described by different types of literature FFs as illustrated in Figure 3. Generic Lennard-Jones (LJ) potential based FFs include UFF[45], Dreiding[46] and AMBER[47]. System specific FFs that use LJ include GenericMOFs[48] and ZhouFF[49]. GenericMOFs is a hybrid FF consisting of Dreiding LJ parameters to describe the methyl-imidizolate linker and UFF LJ parameters to describe the Zn atom. Similarly, ZhouFF uses OPLS-AA[50] LJ parameters for the methyl-imidazolate complex and Dreiding LJ parameters for the Zn atom[12]. Apart from the LJ-based FFs, a couple of Buckingham potential based FFs, namely the MM3 FF (as implemented on RASPA2[48]) and MOF-FF[51] have also been used to describe the ZIF-8 framework. The governing potential equations for both these FFs, as seen in Figure 3 are different adapta-

tions of the original MM3 FF developed by Allinger et.al.[52] (see equation S1 in Supporting Information).

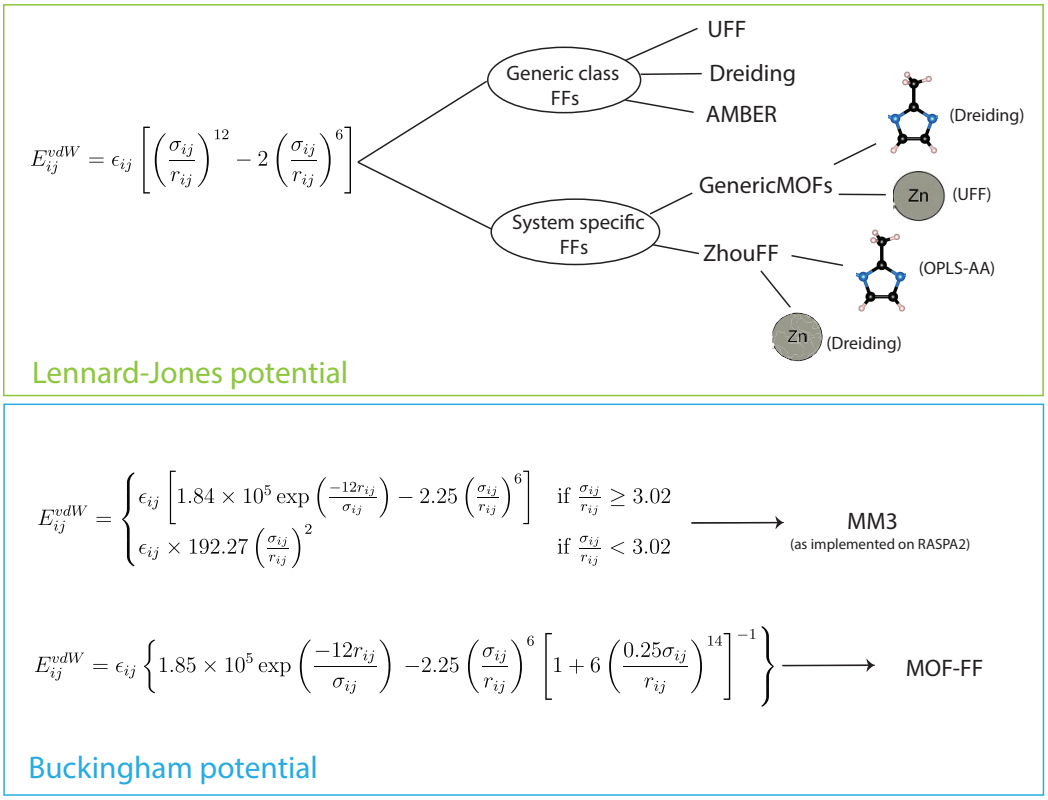

Figure 3: Overview of the different types of literature force fields used in this work to describe the ZIF-8 framework; E_{ij}^{vdW} represents the van der Waals potential between atoms i and j, ϵ_{ij} represents the vdW well depth, σ_{ij} represents the vdW minimum distance and r_{ij} represents the interatomic distance.

When the ZIF-8 framework is described using the LJ-based FFs, the guest molecules are described using the LJ based TraPPE-United Atom (TraPPE)[18] FFs, as is common in literature[13,15,17]. On the other hand, when the ZIF-8 framework is described using the MM3 or MOF-FF FFs, the MM3 all-atom FF parameters are used to describe the guest molecules. The vdW parameters for the various FFs are reported in S2.1 of Supporting Information. The Lorentz-Berthelot mixing rule was used to compute the cross-interaction parameters between the guests and host. The mixing rules were used to compute the guest-guest cross interaction parameters for the MM3 all-atom FFs as well. In this work, the label FF1/FF2 is used to represent the paired literature FFs; where FF1 is used for the FF parameters for

ZIF-8 while FF2 is used for the guest molecule (ethane/ethene).

The electrostatic interactions between ZIF-8 and ethane/ethene molecules were ignored as per previous GCMC studies on ethane/ethene in ZIF-8[42]. This is a reasonable assumption since alkanes and alkenes are usually assumed to be non-polar molecules as we tested by comparing simulated isotherms with/without Coulomb interactions in Section S2.2 of the Supporting Information.

2.2 GCMC simulations

The single component adsorption isotherms and density distribution contours of ethane and ethene in ZIF-8 in this work were obtained using grand canonical Monte Carlo (GCMC) simulations with the RASPA2 package[48]. In the simulations, the common GCMC moves, translation, rotation, reinsertion and swap were considered with equal probabilities. A cut-off radius for the non-bonding interactions of 12.0 Å was used. No tail corrections were applied. Periodic boundary conditions were applied across all dimensions. A supercell containing 8 (2x2x2) unit cells was considered. Each simulation consists of an initial 100,000 cycles for equilibration and subsequent 200,000 cycles for ensemble averages. To compare the simulation results with the experimental uptake, the absolute adsorption uptake obtained from simulations needed to be converted to excess uptake. The details of the procedure to calculate the excess uptake are included in Section S3.4 of Supporting Information.

To validate these simulation settings, previously computed adsorption isotherms of ethane and ethene in ZIF-8 at 298K[43] using the Hertäg force field[53] were recomputed with our settings (see Section S3.1 of Supporting Information).

2.3 Widom Insertion simulations

The Henry coefficients and adsorption enthalpies at infinitely low loading across different FFs were computed using the Widom Insertion (WI) method[54]. This method involves the random insertion of a single guest adsorbate molecule into ZIF-8 and the subsequent computation of

the corresponding interaction energy ΔE as expressed below:

$$\Delta E = E_{ZIF8+guest} - E_{ZIF8} - E_{guest} \tag{1}$$

Combining all samples of the Widom Insertion simulation, the Henry constant and adsorption enthalpy could be extracted as follows:

$$K_H = \frac{\beta}{N} \sum_{i=1}^{N} e^{-\beta \Delta E_{(i)}} \tag{2}$$

$$\Delta H = \frac{\sum_{i=1}^{N} \Delta E_{(i)} \cdot e^{-\beta \Delta E_{(i)}}}{\sum_{i=1}^{N} e^{-\beta \Delta E_{(i)}}} - \frac{1}{\beta} \tag{3}$$

where $\beta = \frac{1}{k_b T}$, N refers to the total number of samples considered for the simulation. The WI calculations were performed using RASPA2[48] and also using the in-house code YAFF[55] with 200,000 WI cycles, which was the same amount of cycles used for the GCMC calculations to generate the adsorption isotherms.

2.4 *Ab initio* calculations at the DFT level

To further validate computational results with experimental results, *ab initio* calculations were performed using Density Functional Theory (DFT) with two different functionals, i.e. PBE- D3(BJ)[56,57] and PBE- MBD[58,59]. The PBE-D3(BJ) functional has been used before[29] to perform importance sampling calculations to compute Henry coefficients for methane adsorption in UiO-66. In that work, it was also suggested that including (many-body) dispersion corrections improves the correlation of the predicted *ab initio* Henry coefficients with the experimental results. The MBD method developed by Tkatchenko et al.[58] is widely used to include many-body vdW dispersion interactions in DFT calculations. It is based on correlated quantum harmonic oscillators (QHOs) and it therefore represents a more general and less empirical approach as compared to DFT-D3 for instance[60]. MBD is grounded in the random-phase approximation (RPA), based on the adiabatic connection fluctuation-

dissipation theorem (ACFDT)[61]. Concretely, the MBD expression is formally equivalent to the RPA correlation energy for a system of QHOs in the dipole approximation, which gives it clear ab initio origins and is not very empirical[62]. It was observed that the low loading properties (i.e. Henry coefficients and adsorption enthalpies at infinitely low loading) derived from simulations using the PBE-MBD functional closely matches the experimental results, justifying its choice for the subsequent calculations over the PBE-D3(BJ) level of theory (see Section S4 of Supporting Information).

The periodic single-point DFT calculations were performed using VASP version 6.2[63,64] using the projector augmented wave (PAW) method[65] with the supplied PAW-PBE potentials. A plane wave cutoff of 900 eV was used for the ZIF-8/ethane and ethene systems while a cutoff of 800 eV was used for the ZIF-8/propane and propene systems. Due to the large unit cell length of 16.99 Å for the ZIF-8 framework, only the gamma point was used to sample the Brillouin zone. Previous DFT studies involving the ZIF-8 framework have used similar input parameters[66].

For the importance sampling experiments involving ZIF-8/ethane and ethene, a total of 1000 *ab initio* calculations were sufficient while a slightly larger number of 1400 and 1200 were required for the ZIF-8/propane and ZIF-8/propene systems respectively. To ensure that the number of samples chosen were sufficient to sample the *ab initio* potential energy surface, a convergence test was performed (see Section S4 of Supporting Information).

2.5 Importance sampling methodology

The overview of the importance sampling methodology is illustrated in Figure 4. The first step of the importance sampling methodology involves using the Widom insertion method with a FF to generate a random set of N configurations with corresponding FF potentials ($\Delta E^{FF}_{(1)}, \Delta E^{FF}_{(2)}, \Delta E^{FF}_{(3)}, \ldots, \Delta E^{FF}_{(N)}$), which allows to extract an estimate for the Henry coefficient K^{FF}_H.

In the second step, we repeatedly propose a random sample taken from the WI pool, as

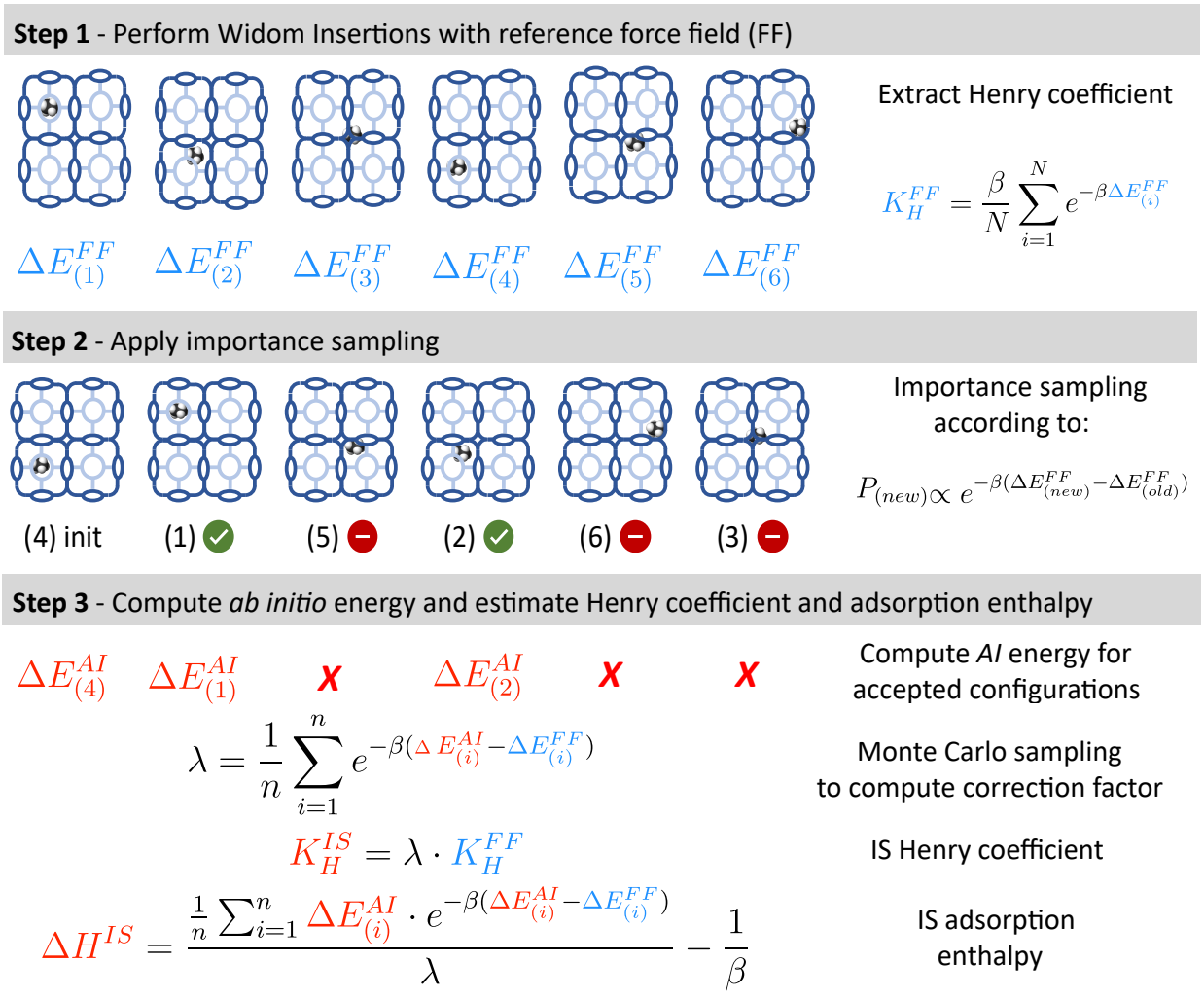

Figure 4: Overview of the importance sampling methodology; K_H^{FF} and K_H^{IS} refers to the force field and importance sampling derived Henry coefficient, $\Delta E_{(i)}^{FF}$ and $\Delta E_{(i)}^{AI}$ refers to the FF and *ab initio* derived potential for configuration i, $\beta = \frac{1}{k_b T}$, λ refers to the correction factor, N refers to the number of configurations considered for Widom Insertion while n refers to the number of configurations considered for computing the correction factor; in step 2, $P(new)$ refers to the acceptance probability of a new configuration while $\Delta E_{(new)}^{FF}$ and $\Delta E_{(old)}^{FF}$ refer to the force field derived potentials of the new and old configurations respectively; in step 3, the red crosses symbolize the configurations that were rejected by the importance sampling procedure for which no *ab initio* calculations were performed.

defined by its index in the pool instead of having to come up with viable positions of all atoms. Such random configurations will then either be accepted as the new configuration or rejected, in which case, the old configuration remains in place. "new" represents the configuration that is being evaluated to determine whether or not we will accept it or not. "old" represents the current configuration of the system. The acceptance/rejection is decided based on the Boltzmann factor with the FF energy. Whenever a configuration is accepted, we need to compute its contribution to the λ correction factor, which means we need to compute its *ab initio* energy. If a configuration is rejected, we again account for the contribution to the λ correction factor according to the old configuration.

In this context, the fact that the order of the sampled configurations is 'reordered' just represents the fact that the initial ("init") configuration was randomly picked. Picking a different "init" configuration will not affect the importance sampling result as long as sufficient n samples are chosen to determine the Henry coefficient for the importance sampling methodology. We then determine the acceptance probability of selecting a configuration and this is done according to the Boltzmann probability distribution:

$$P_{(new)} \propto e^{-\beta(\Delta E^{FF}_{(new)} - \Delta E^{FF}_{(old)})} \tag{4}$$

where $\Delta E^{FF}_{(new)}$ and $\Delta E^{FF}_{(old)}$ refer to the force field derived potentials of the newly considered configuration and current configuration respectively. A total of n configurations is selected for the subsequent step of *ab initio* calculations. The choice of n is dependent on various parameters involving system size, identity of the adsorbent framework and adsorbate molecules. Typically, the choice of n should be kept to a minimum to avoid expending large computational resources since an *ab initio* calculation is orders of magnitude more computationally expensive than a FF calculation. To evaluate the choice of n configurations, we provide a systematic approach to understand the convergence behaviour of the system. We evaluate the Henry coefficient and adsorption enthalpy for the first 50 configurations, then

for the first 100 and then the first 150 and so on. When the difference between the consecutive evaluations are below the threshold of 1% of the Henry coefficient and 0.1% of the adsorption enthalpy, the minimum number of configurations required to achieve convergence has been obtained (n). Section S4 of Supporting Information provides further details as to how n was determined for the test cases of ZIF-8/ethane and ethene. n was determined to be 1000 for the test cases of ZIF-8/ethane and ethene.

The geometries of the host-guest complex are then supplied as input to the *ab initio* calculations performed in the next step. The *ab initio* energies obtained from the DFT calculations which can be performed using any external software package can then be used to compute the scaling factor for the FF derived Henry coefficient K_H^{FF} and adsorption enthalpy ΔH^{FF} which is expressed as follows:

$$\lambda = \frac{1}{n}\sum_{i=1}^{n} e^{-\beta(\Delta E_{(i)}^{AI} - \Delta E_{(i)}^{FF})} \tag{5}$$

The importance sampling (IS) Henry coefficient, K_H^{IS}, and adsorption enthalpy at infinitely low loading ΔH^{IS} can now be computed as follows:

$$K_H^{IS} = \lambda \cdot K_H^{FF} \tag{6}$$

$$\Delta H^{IS} = \frac{\frac{1}{n}\sum_{i=1}^{n} \Delta E_{(i)}^{AI} \cdot e^{-\beta(\Delta E_{(i)}^{AI} - \Delta E_{(i)}^{FF})}}{\lambda} - \frac{1}{\beta} \tag{7}$$

The convergence of the IS procedure depends on the similarity of the FF and *ab initio* PES. To achieve convergence, it was also imperative that an adequate number of samples are included to ensure that the *ab initio* potential energy surface is adequately sampled as this would directly affect the accuracy of results. The convergence test results are shown in Section S4 of Supporting Information.

The standard entropy of adsorption at a very low but finite uptake region with P $\rightarrow$ 0 could be estimated with K_H, ΔH and the free pore volume of the ZIF-8 framework, V_{free},

as expressed below[67]:

$$\Delta S \approx \frac{\Delta H}{T} + R \ln \frac{K_H RT}{V_{free}} \tag{8}$$

where T represents the system temperature and R represents the gas constant.

2.6 Numerical metric to compare simulation and experimental results

To validate the performance of a FF in its ability to reproduce the experimental adsorption isotherm, an uptake disparity metric was introduced to measure the difference between two adsorption isotherms. This metric was evaluated as illustrated in Figure 5 and equation 9 where S(P) represents the function describing the FF uptake against pressure while E(P) represents the function describing the experimental uptake against pressure.

$$U^{disp} = \int_a^b \frac{1}{b-a} \frac{S(P) - E(P)}{E(P)} dP \times 100\% \tag{9}$$

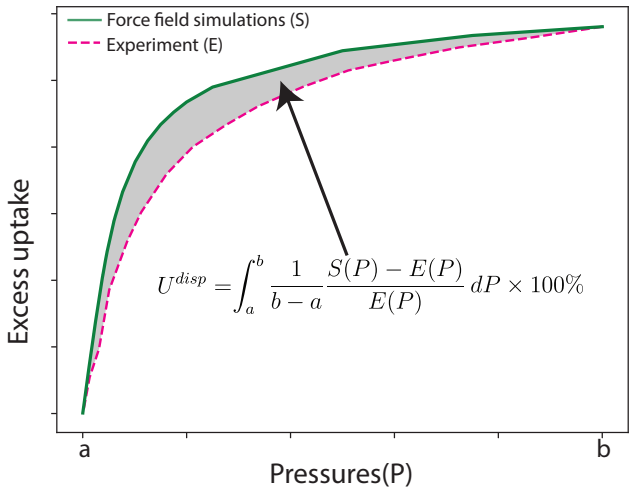

Figure 5: A generic isotherm plot illustrating the calculation of the uptake disparity between force field simulation and experimental isotherms across a pressure interval.

In order to compute the area between the FF simulated isotherm and the experimental isotherm, a polynomial expression was fitted to the data point set of both isotherms to

have a mathematical function available for both. The area between both curves can then easily be estimated numerically using gaussian quadrature (see Section 3.6 of Supporting Information). In this work, this uptake disparity metric was applied across a pressure range of 0.001 to 1 bar.

Apart from comparing uptakes between adsorption isotherms, the FF derived Henry coefficients K_H^{FF} were compared with a quantum accurate reference henry coefficient, $K_H^{IS\_ref}$, computed using the importance sampling methodology. This disparity, $K_{\mathrm{H}}^{\mathrm{disp}}$, is calculated as follows:

$$K_{\mathrm{H}}^{\mathrm{disp}} = \frac{K_{\mathrm{H}}^{\mathrm{FF}} - K_{\mathrm{H}}^{IS\_ref}}{K_{\mathrm{H}}^{IS\_ref}} \times 100\% \tag{10}$$

2.7 Experimental methods

2.7.1 Chemicals

Commercial ZIF-8 was supplied by Sigma-Aldrich. Highly pure helium (99.99%), ethane (99.95%), ethene (99.95%), propane (99.95%) and propene (99.95%) were acquired from Air Liquide.

2.7.2 Pulse IGC experiments

The performance of ZIF-8 for the adsorptive separation of ethane, ethene and propane, propene in the low coverage region was estimated using an in-house customized inverse gas chromatography instrument (based on an Agilent technologies 7820A gas chromatograph). The detection of hydrocarbons was achieved by a Flame Ionization Detector (FID).

A stainless-steel column (L= 10 cm and ID= 0.216 cm) was filled with adsorbent pellets to prohibit a high pressure-drop in the column. Hence, pelletization was achieved by compressing adsorbent powder with a mechanical press, followed by crushing and sieving to obtain pellets with a size range between 250μm and 500μm.

Prior to pulse IGC experiments, the prepared column was activated overnight at 250°C using designed thermal ramps under a helium flow (Table 1). A small pulse of an intended gas

Table 1: The thermal ramps for the activation of ZIF-8.

Ramps	Temperature (°C)	Rate (°C/min)	Hold time (min)
1	80	2	10
2	120	1	30
3	250	2	900

was injected using a Hamilton syringe (CR-700). Helium was used as the carrier gas at the flow of 15 Nml/min. In order to estimate thermodynamic parameters, each gas was injected within a temperature range of 30-80°C with 10°C intervals. The dead time was quantified through zero-length column experiments and obtained values were subtracted from the first order moment. Three repetitions were conducted, and the average value was considered for calculations.

The Henry constants ($K_H^{exp\_ref}$) were calculated using the first order moment of chromatograms and adsorption enthalpies and entropies were determined from the temperature dependency of the Henry constants, using the van 't Hoff equation.

2.7.3 Measurement of adsorption isotherms

Single gas adsorption isotherms for ethane, ethene and propane, propene on ZIF-8 were obtained via a volumetric approach by an Autosorb AS-1 (Quantachrome Instruments, USA) device equipped with an oil bath to stabilize temperature. Using programmed thermal ramps, the activation temperature slowly increased up to 250°C and ZIF-8 was vacuum-activated overnight. The isotherms of nitrogen in outgassed ZIF-8 were measured at 77 K.

3. Results and Discussion

3.1 Benchmarking force field based GCMC isotherms with experiment

The performance of the literature force fields' predictions across different pressure regimes was evaluated based on the numerical disparity metrics discussed previously against experimental isotherms developed according to the methodology of Section 2.6.

Figures 6 (a) and (b) show the simulated and experimental single-component adsorption isotherms of ZIF-8/ethane and ZIF-8/ethene respectively in the low pressure regime, between 0.001 to 1.0 bar, at 303K. As the disparities between FF and experimental isotherms were larger in the low pressure range, these isotherms were included in the main manuscript while the full simulated isotherm plots across the various literature FFs are included in Figure S11 of the Supporting Information. It can be observed that there is no single literature

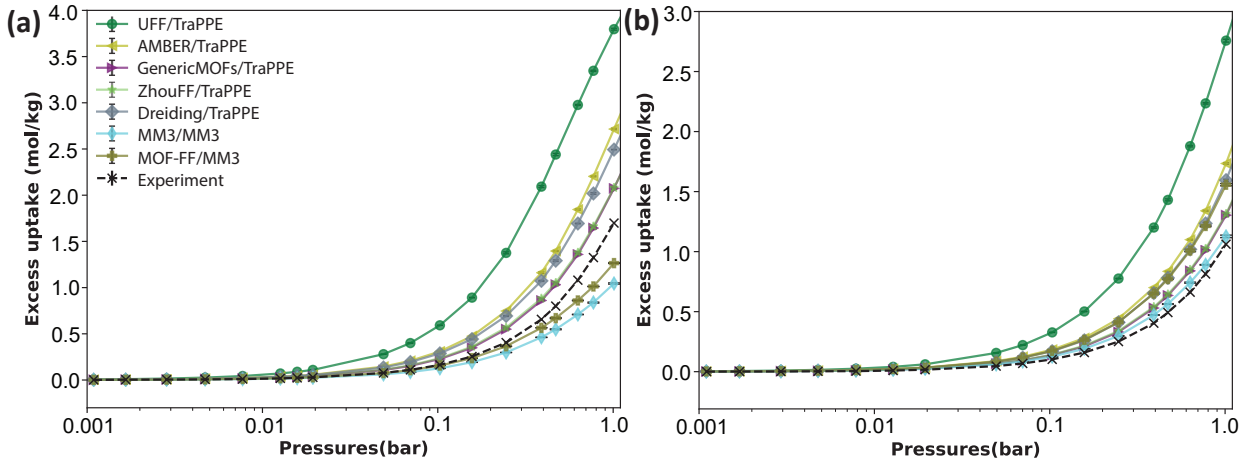

Figure 6: (a) Adsorption isotherms for ZIF-8/ethane and (b) for ZIF-8/ethene from various literature FFs compared with experiments at 303K across a pressure range of 0.001 to 1.0 bar. The label FF1/FF2 is used to represent the literature force fields; where FF1 is used for the FF parameters for ZIF-8 while FF2 is used for the adsorbate molecule.

FF that could match the experimental results across the two adsorbates. All LJ-based FFs are observed to overestimate the experimental isotherm to various extents. The predictions of the Buckingham-based FFs were observed to vary according the identity of the guest

molecule. The MM3/MM3 isotherm underestimates the experimental isotherm for ethane while overestimating for ethene. MOF-FF/MM3 matches the experimental isotherm for ethane while significantly overestimating for ethene. To go beyond a qualitative analysis of the FF isotherms' agreement with the experimental isotherms, the uptake disparities, U^{disp}, of the various literature FFs with respect to experimental results are tabulated in Table 2.

Table 2: Uptake disparities with respect to experimental results across different literature force fields in the low pressure regime.

Guest molecules	**Host/guest FF**	$U^{disp}(\%)$
Ethane	MOF-FF/MM3	-16
	GenericMOFs/TraPPE	29
	MM3/MM3	-29
	ZhouFF/TraPPE	32
	Dreiding/TraPPE	60
	AMBER/TraPPE	74
	UFF/TraPPE	197
Ethene	MM3/MM3	28
	GenericMOFs/TraPPE	29
	ZhouFF/TraPPE	31
	Dreiding/TraPPE	59
	MOF-FF/MM3	60
	AMBER/TraPPE	71
	UFF/TraPPE	194

It could be observed that there was a decent quantitative agreement of the MM3/MM3 FF across both guest molecules and MOF-FF/MM3 FF for ethane. However, both FF isotherms predict that ethene uptake is higher than that of ethane in ZIF-8 for the same pressure. This is an incorrect qualitative prediction since the experimental results clearly indicate that the uptake of ethane is greater than that of ethene in ZIF-8 at the same pressure which is consistent with the observation that ZIF-8 is a paraffin selective MOF[44]. Despite the wide variations in quantitative predictions of uptake, all LJ-based FFs correctly predict the qualitative trend in uptake between ethane and ethene in ZIF-8 unlike the Buckingham-based FFs. Therefore, for these specific systems, the predictions of the LJ-based FFs are

deemed to be more reliable than that of the Buckingham-based FFs.

Only considering the LJ-based FFs, the isotherms estimated with FFs that were derived specific for the system at hand, the so called system specific FFs, such as GenericMOFs/TraPPE and ZhouFF/TraPPE were observed to have significantly better agreement with experimental isotherms than the generic class FFs as observed from Table 2. Both GenericMOFs/TraPPE and ZhouFF/TraPPE, have on average, approximately 30% lower disparity than the best performing generic class FF in Dreiding/TraPPE. This is along expected lines as the system specific FFs have distinct parameters for the methyl-imidazolate complex in ZIF-8 while this is not the case for the generic FFs. These modifications were an attempt to better correlate with experimental results.

Nevertheless, even these system specific FFs are observed to have their limitations in the low pressure regime where disparities are still around 30%. To analyze the reasons behind this significant disparity, it is instructive to look at the LJ potential expression as seen in Figure 3. The r^{-12} term in the LJ expression approximates the strong Pauli repulsion originating from overlap of electron orbitals. However, this repulsive term is known to be a crude approximation of exponentially decaying repulsive interactions and usually overestimates what is observed in experiments as well as *ab initio* calculations[51]. Furthermore, the uptake at low pressure regimes is proportional to the Boltzmann factor, which means that errors on the repulsive energy are amplified slightly in the corresponding predicted uptake by the LJ-based FFs[23].

3.2 Defining the reference Henry coefficient with PBE-MBD using importance sampling

To accurately capture the host-guest interactions at the low-pressure regime, a Henry coefficient reference needs to be obtained. This reference needs to ideally satisfy a number of requirements. Firstly, the results should be invariant of FFs. Secondly, the methodology to obtain the reference needs to be independent of experimental input, however, the results are

required to have a close agreement with experimental results. Lastly, it needs to be obtained with minimal computational overhead. To satisfy these requirements, we generate the reference Henry coefficient $K_H^{IS\_ref}$ through the importance sampling technique[29] (as outlined in Section 2.5). The *ab initio* calculations are performed with the PBE-MBD functional to ensure a close correlation to the experimental results (see Section S4 of Supporting Information). It should be noted that the choice of the most appropriate functional used to perform the *ab initio* calculations is system-dependent. Therefore, it is recommended to perform a benchmark test to choose the appropriate functional for the system at hand.

To prove the FF invariance of the importance sampling refined Henry coefficients, K_H^{IS}, separate importance sampling trials were performed for five different LJ-based FFs. These five LJ-based FFs were observed to have distinctly different uptakes in the adsorption isotherms in Figure 6 in the low pressure regime and are thus ideal to validate the FF invariance hypothesis. The Buckingham-based FFs were excluded from these trials due to a sampling issue resulting from the systematic underestimation of the adsorption affinity (overestimation of the negatively valued adsorption energy) as observed in the MM3/MM3 FF in Figures S5a and S6a. Such underestimation leads to an under-representation in importance sampling of probable configurations, i.e. probable according to the *ab initio* level of theory, which cannot be corrected for as it represents missing configurations. In contrast, if a given FF would give rise to a systematic overestimation of the adsorption affinity (as is the case in UFF/TraPPE seen in Figures S5b and S6b), it gives rise to over-representation of configurations which can be corrected for by importance sampling. More details on this sampling issue, including how to detect it from easy to generate histograms, are included in Section S2.4 of Supporting Information.

Every other parameter such as temperature and *ab initio* calculation parameters were kept constant for the trials. In Table 3, the results were compared with the experimental derived Henry coefficients, $K_H^{exp\_ref}$ and adsorption enthalpies, ΔH^{exp_ref}, at infinitely low loading.

Table 3: Summary of importance sampling (IS) results across different force fields for ZIF-8/ethane and ethene at 303K.

Guest	**Host/guest FF**	K_H^{IS}, $K_H^{exp\_ref}$ **(mol/kg/bar)**	ΔH^{IS}, ΔH^{exp_ref} **(kJ/mol)**	ΔS^{IS}, ΔS^{exp_ref} **(kJ/K/mol)**
Ethane	UFF/TraPPE	1.717 ± 0.381	-18.99 ± 1.28	-0.0260 ± 0.0042
	Dreiding/TraPPE	1.731 ± 0.405	-19.02 ± 1.26	-0.0260 ± 0.0042
	AMBER/TraPPE	1.748 ± 0.345	-18.91 ± 1.36	-0.0256 ± 0.0045
	GenericMOFs/TraPPE	1.833 ± 0.479	-19.32 ± 1.52	-0.0265 ± 0.0050
	ZhouFF/TraPPE	1.998 ± 0.460	-19.01 ± 1.64	-0.0248 ± 0.0054
	Average	1.806	-19.05	-0.0260
	Experiment	1.888 ± 0.008	-19.50 ± 0.10	-0.0269 ± 0.0003
Ethene	UFF/TraPPE	1.277 ± 0.270	-18.20 ± 1.32	-0.0258 ± 0.0040
	Dreiding/TraPPE	1.260 ± 0.269	-18.02 ± 1.23	-0.0253 ± 0.0041
	AMBER/TraPPE	1.423 ± 0.281	-18.39 ± 1.40	-0.0256 ± 0.0046
	GenericMOFs/TraPPE	1.266 ± 0.232	-17.91 ± 1.28	-0.0249 ± 0.0042
	ZhouFF/TraPPE	1.397 ± 0.407	-18.28 ± 1.48	-0.0253 ± 0.0049
	Average	1.325	-18.16	-0.0250
	Experiment	1.193 ± 0.006	-17.70 ± 0.20	-0.0247 ± 0.0007

From Table 3, it can be observed that K_H^{IS}, ΔH^{IS} and ΔS^{IS} originating from various initial FFs lie within the error margins of each other. There is a maximum deviation of only 14% (ethane), 11% (ethene) for K_H^{IS}, 2% (ethane), 3% (ethene) for ΔH^{IS} and 7% (ethane), 4% (ethene) for ΔS^{IS}. Further, the average Henry coefficient of the five initial FFs deviate 5% (ethane) and 11% (ethene) from experimental results. This proves both the invariance towards the initial FF used to start the importance sampling technique and good agreement with experimental results. This makes K_H^{IS} ideal in terms of benchmarking literature FFs in the low pressure regime. Among the five K_H^{IS}, the Henry coefficient with the least absolute difference to the average Henry coefficient was chosen to be the reference Henry coefficient. In all fairness, the choice of the tested FF does not matter too much in determining the reference Henry coefficient as shown in Section S2.5 of Supplementary Information. For the ZIF-8/ethane system, the GenericMOFs/TraPPE importance sampling Henry coefficient of 1.833 mol/kg/bar and for the ZIF-8/ethene system, the UFF/TraPPE importance sampling Henry coefficient of 1.277 mol/kg/bar were chosen as reference Henry coefficients, $K_H^{IS\_ref}$

which will be used to develop two methodologies.

3.3 Benchmarking the force field derived Henry coefficient with the reference Henry coefficient

The first methodology involves comparing K_H^{FF} with $K_H^{IS\_ref}$ and introduce a ranking of FFs based on the Henry coefficient disparity, K_H^{disp}, as expressed in equation 10. The Henry region in the adsorption isotherm is characterized by a linear uptake as a function of pressure. The Henry coefficient, which is the gradient in this linear regime, completely characterizes the adsorption properties of a system in this low pressure regime. Therefore, the relative disparity between K_H^{FF} and $K_H^{IS\_ref}$ has an important predictive power in assessing the accuracy of simulated adsorption isotherms in the low pressure regime.

K_H^{FF} can be obtained for each trial FF from the Widom insertion simulations as described in Section 2.3. $K_H^{IS\_ref}$ can be obtained from the importance sampling methodology as described in Section 2.5. FFs are ranked in ascending order according to K_H^{disp}, such that FFs with larger K_H^{disp} receiving lower rankings.

The results for the ZIF-8/ethane and ethene system at 303K are tabulated in Table 4. Comparing Table 4 and Table 2 which describes the uptake disparities, U^{disp}, of the FFs with respect to experimental isotherms, it can be observed that the ranking of the FFs are similar. This means that the benchmarking methodology is observed to predict the ranking of FF isotherms with respect to experimental isotherms at the low pressure regime accurately. Furthermore, K_H^{disp} and U^{disp} have close agreement across all the FFs investigated. This therefore validates the benchmarking methodology for literature FFs.

Since the benchmarking methodology is based on Henry coefficients, which are a description of the host-guest interactions, it is expected that its predictive power is at its greatest in regions of the adsorption isotherm where the host-guest interactions are predominant, at lower pressure regimes. This is indeed confirmed in Figure S12 in Section S3.5 of Supporting Information, which is a plot of host-guest and guest- guest interaction contributions against

Table 4: Benchmarking results for literature force fields with importance sampling reference Henry coefficients for ZIF-8/ethane and ethene at 303K; Henry coefficients and adsorption enthalpies at infinitely low loading are derived using the Widom Insertion[54] method (see section 2.3).

Guest	**Host/guest FF**	K_H^{FF} **(mol/kg/bar)**	$K_H^{IS\_ref}$ **(mol/kg/bar)**	$K_H^{disp}(\%)$
Ethane	MOF-FF/MM3	1.566 ± 0.003	1.833	-15
	GenericMOFs/TraPPE	2.179 ± 0.003		19
	ZhouFF/TraPPE	2.271 ± 0.004		24
	MM3/MM3	1.259 ± 0.002		-31
	Dreiding/TraPPE	2.744 ± 0.004		50
	AMBER/TraPPE	2.937 ± 0.005		60
	UFF/TraPPE	5.602 ± 0.007		206
Ethene	GenericMOFs/TraPPE	1.334 ± 0.001	1.277	4
	MM3/MM3	1.216 ± 0.002		-5
	ZhouFF/TraPPE	1.371 ± 0.001		7
	Dreiding/TraPPE	1.649 ± 0.002		29
	MOF-FF/MM3	1.706 ± 0.003		34
	AMBER/TraPPE	1.761 ± 0.002		38
	UFF/TraPPE	3.145 ± 0.003		146

pressure. However, the figure also indicates that the host-guest interactions are responsible for as much as 85% of the total interaction energy near the saturation uptake region at 10 bar. This illustrates that this methodology would still have adequate predictive power in higher pressure regimes for these systems. This notion leads us to our second methodology which makes use of $K_H^{IS\_ref}$ to rescale FFs to provide better agreement with experimental isotherms not only at low pressure regimes but also potentially for the entire pressure range.

3.4 Rescaling force field parameters to obtain better isotherms

Apart from benchmarking literature FFs, the $K_H^{IS\_ref}$ could also be used to generate a rescaled FF that has close agreement with the experimental results at the very least in the low pressure regime. However, given the high contribution of host-guest interactions in the saturation regime, it might also be anticipated that such rescaled FFs reproduce the experimental isotherm in the medium and higher pressure regimes.

As seen in Table 2, in the low pressure regime, all five of the generic LJ-based FFs overestimate uptake as compared to the experimental isotherm. Figure S4 in Section S2.3 of Supporting Information depicts a plot of short-range interaction energies against interatomic radius between two sp^3 hybridized carbons across different generic LJ-based FFs. Among the various FFs, UFF is observed to have the highest attractive effect as represented by having the greatest absolute minimum in interatomic energy. In general, comparing Figure S4 to Table 2, we can see the absolute minimum in interatomic energy has a correlation with the overestimation in uptake. For instance, UFF strongly overestimates the uptake compared to experiments, which is correlated with the strongest minima of the interatomic energy. Therefore, the FF can be made less attractive by uniformly rescaling the epsilon parameters of the framework atoms such that the new FF predicts a Henry constant matching the reference. A similar FF rescaling procedure has been performed before in literature but the reference results used in these works were solely based on experimental adsorption isotherms[26–28].

This guided search would result in a FF that can be considered as an adequate theoretical description of the host-guest interactions in the low loading regime. Since the guest-guest interactions are adequately described by TraPPE, the guest adsorbate molecules will remain described by TraPPE. It is to be emphasised that this systematic FF rescaling methodology is not an adhoc tweak to match the experimental results. This rescaling methodology can be envisioned to apply a quick correction to any available LJ-based FF describing the host framework to improve the low loading interactions on average. As mentioned in Section 3.1, since the qualitative predictions of the Buckingham-based FFs were off, these FFs were not considered to be suitable candidates to apply this methodology.

The epsilon parameter of the ZIF-8 framework atoms of the FFs were systematically and uniformly reduced, while keeping the sigma parameters unaltered, until the WI Henry coefficient matches $K_H^{IS\_ref}$ as seen in Table 5. The parameters of the rescaled FFs are reported in Table S3 of Supporting Information.

Table 5: Rescaling factor applied to epsilon parameters such that the force field Henry coefficient matches the reference.

Guest molecules	Host/guest FF	Reduced ϵ
Ethane	UFF/TraPPE	$0.73\varepsilon_{\text{UFF}}$
	AMBER/TraPPE	$0.87\varepsilon_{\text{AMBER}}$
	Dreiding/TraPPE	$0.89\varepsilon_{\text{Dreiding}}$
	ZhouFF/TraPPE	$0.94\varepsilon_{\text{ZhouFF}}$
	GenericMOFs/TraPPE	$0.95\varepsilon_{\text{GenericMOFs}}$
Ethene	UFF/TraPPE	$0.75\varepsilon_{\text{UFF}}$
	AMBER/TraPPE	$0.89\varepsilon_{\text{AMBER}}$
	Dreiding/TraPPE	$0.91\varepsilon_{\text{Dreiding}}$
	ZhouFF/TraPPE	$0.97\varepsilon_{\text{ZhouFF}}$
	GenericMOFs/TraPPE	$0.98\varepsilon_{\text{GenericMOFs}}$

These rescaled FFs were then used to generate adsorption isotherms with GCMC simulations with similar settings to the earlier simulations. Figures 7 (a) and (b) show the rescaled and experimental single-component adsorption isotherms of ethane and ethene in ZIF-8 respectively in the low pressure regime, between 0.001 to 10.0 bar. To evaluate the agreement of the rescaled FF isotherm at higher pressures, experimental isotherm data at 298K, from Bux et.al.[68], is provided for reference. Accordingly, to effectively compare against this isotherm, we included the rescaled FF isotherm simulated at 298K.

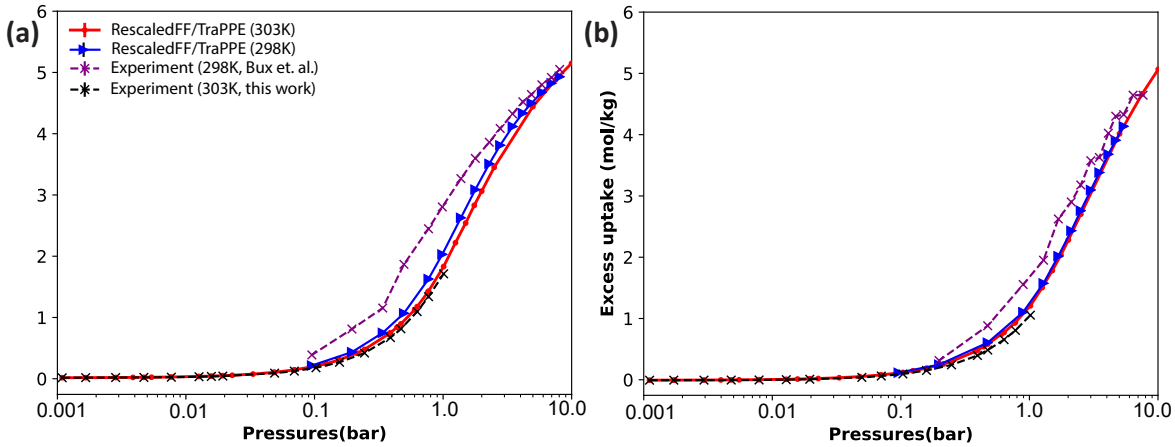

Figure 7: (a) Comparison of rescaled force fields and experimental isotherms at 298K and 303K for ZIF-8/ethane and (b) ZIF-8/ethene between 0.001 and 10.0 bar.

All five rescaled FFs were found to produce similar isotherms with similar uptakes. There-

fore, only the isotherm of the rescaled UFF/TraPPE has been included in Figure 7. To analyze the numerical disparities across the different rescaled FF and experimental isotherms, Table 6 describes U^{disp}.

Table 6: Uptake disparities with respect to experimental results across different rescaled force fields, simulated at 303K and the rescaled UFF/TraPPE force field simulated at 298K. The uptake disparities at low pressure (0.001 to 1 bar) are compared against experimental results from this work while the uptake disparities at the medium-high pressure regimes are compared against experimental isotherms from literature at 298K[68]

Guest	**Host/guest FF**	U^{disp}(%) [303K] (0.001 to 1 bar)	U^{disp}(%) [298K[68]] (0.1 to 8.1 bar)
Ethane	Rescaled ZhouFF/TraPPE	9	-
	Rescaled UFF/TraPPE	11	-13
	Rescaled GenericMOFs/TraPPE	11	-
	Rescaled Dreiding/TraPPE	11	-
	Rescaled AMBER/TraPPE	12	-
Ethene	Rescaled AMBER/TraPPE	20	-
	Rescaled Dreiding/TraPPE	20	-
	Rescaled ZhouFF/TraPPE	21	-
	Rescaled GenericMOFs/TraPPE	21	-
	Rescaled UFF/TraPPE	21	-9

The invariance in adsorption isotherms across the rescaled FFs confirms that the methodology is working as expected. Since the K_H^{FF} of the FFs is matched to that of $K_H^{IS\_ref}$, the U^{disp} of the FFs at the low pressure regime is similar. Furthermore, improving the K_H^{FF} to match $K_H^{IS\_ref}$ also results in a corresponding improvement of ΔH^{FF}. For ethane and ethene, ΔH^{FF} of the rescaled FF are -17.3 kJ/mol and -16.0 kJ/mol respectively. Both values are within 2.0 kJ/mol of ΔH^{IS_ref} of -19.3 kJ/mol and -18.0 kJ/mol for ethane and ethene respectively. The convergence in the adsorption enthalpy and Henry coefficients ensured that the description of the host-guest interactions are similar across the five rescaled FFs. Furthermore, since the guest-guest interactions are described by TraPPE for all five FFs, the isotherms are observed to be similar. Therefore, this means that the rescaling methodology could be applied across any LJ-based FF describing the host framework with TraPPE used to describe the guest and a similar result would be obtained. Across the medium and higher

pressure regime of 0.1 bar to 8.1 bar, the rescaled UFF/TraPPE FF isotherm is observed to have good agreement with the experimental isotherm with a U^{disp} of only -13% and -9%. Although the rescaled FF was specifically developed for the lower pressure regimes, it has reasonable agreement with the literature isotherm. This means that the FF rescaling methodology has reasonable predictive power in the higher pressure regimes.

From Figure 7 and from comparing Tables 2 and 6 the rescaled FF isotherms are observed to have better agreement with the experimental isotherms than the other literature LJ-based FF isotherms. When comparing the uptake disparities, the best performing FF for ethane went from having a disparity of -16% to +9% and for ethene from 28% to 20%. This observation is along expected lines since the rescaled FFs provide a better description of the host-guest interactions over the original literature FFs.

The rescaled isotherms report higher U^{disp} for ethene than for ethane. This could be attributed to the marginal overestimation of the $K_H^{IS\_ref}$ to the $K_H^{exp\_ref}$. For ethene, this overestimation stood at 5.6% as compared to ethane at 1.7%. This suggests that the importance sampling methodology is marginally more accurate for ZIF-8/ethane over ZIF-8/ethene.

3.5 Transferability of the FF rescaling methodology to C3 molecules

We investigated the transferability of the FF rescaling methodology to the C3 guest molecules (propane and propene) in ZIF-8. As before, we first define the reference Henry coefficient with PBE-MBD using importance sampling and the results are tabulated in Table 7. UFF/TraPPE was used to perform the FF based Widom Insertion simulations for the importance sampling methodology. From Table 7, it can be observed that K_H^{IS} lies well within the error margin of the experimental results for both the ZIF-8/propane and propene systems. However, ΔH^{IS} and ΔS^{IS} are slightly overestimated with respect to the experimental results. As seen from equation 8, the ΔH^{IS} has a greater influence in the estimate of ΔS^{IS} as compared to K_H^{IS} which is within a natural log operator. Therefore, it is not surprising that a larger error in the estimate of ΔH^{IS} propagates towards a larger error of

Table 7: Importance sampling (IS) and experimental results for ZIF-8/propane and propene at 303K.

Guest	Methodology	K_H^{IS}, $K_H^{exp\_ref}$ (mol/kg/bar)	ΔH^{IS}, ΔH^{exp_ref} (kJ/mol)	ΔS^{IS}, ΔS^{exp_ref} (kJ/K/mol)
Propane	IS	11.148 ± 3.410	-25.15 ± 1.41	-0.0308 ± 0.0047
	Experiment	11.638 ± 0.410	-27.80 ± 0.10	-0.0391 ± 0.0003
Propene	IS	9.586 ± 2.719	-23.85 ± 1.52	-0.0277 ± 0.0050
	Experiment	9.052 ± 0.290	-27.40 ± 0.10	-0.0399 ± 0.0003

the corresponding ΔS^{IS} estimate. Nevertheless, the close agreement of the K_H^{IS} with the experiment, with which the proposed methodologies are based upon, indicates the possible transferability of the methodology to the C3 molecules.

Next, the epsilon parameter of the ZIF-8 framework atoms of the UFF/TraPPE FF was systematically and uniformly reduced, while keeping the sigma parameters unaltered, until the WI Henry coefficient matches K_H^{IS} as seen in Table 8. The exact FF parameters are reported in Table S3 of Supporting Information. Figure 8 (a) and (b) show the literature,

Table 8: Rescaling factor applied to epsilon parameters such that the force field Henry coefficient matches the reference.

Guest molecules	Host/guest FF	Reduced ϵ
Ethane	UFF/TraPPE	$0.77\varepsilon_{\text{UFF}}$
Ethene	UFF/TraPPE	$0.81\varepsilon_{\text{UFF}}$

rescaled and experimental single-component adsorption isotherms of propane and propene in ZIF-8 respectively in the pressure regime, between 0.001 to 1.0 bar at 303K. Similar to the case with the C2 molecules, it is observed that the rescaled UFF/TraPPE isotherm has significantly closer agreement with the experimental isotherm as compared to the original UFF/TraPPE isotherm for both propane and propene. It can also be observed that the system-specific FFs in GenericMOFs/TraPPE and ZhouFF/TraPPE have closer agreement to the experimental isotherm than the generic FFs and also the rescaled UFF/TraPPE isotherm. To analyze the numerical disparities across the different isotherms, Table 9 describes U^{disp}. As observed from Figure 8, it can be observed that for both propane and

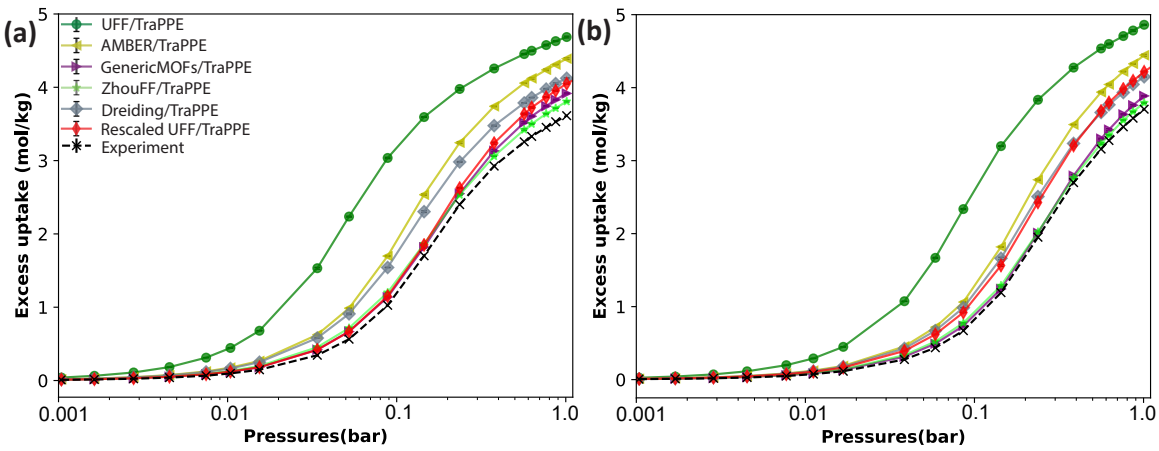

Figure 8: (a) Comparison of experimental isotherms with literature and rescaled force field isotherms for ZIF-8/propane and (b) ZIF-8/propene between 0.001 and 1.0 bar.

propene, ZhouFF/TraPPE and GenericMOFs/TraPPE have the closest agreement to the experimental isotherm with U^{disp} below 10%. This is followed by the rescaled UFF/TraPPE isotherm which has a slightly higher disparity of 21% for propene as compared to 12% for propane. This trend is similar to what was observed with ethane and ethene in that U^{disp} was greater for the alkene guest molecule as compared to the alkane guest molecule. This was followed by the generic FFs in Dreiding/TraPPE, AMBER/TraPPE and UFF/TraPPE which is the same order which was observed for the C2 molecules as well. Significantly, the rescaled FF isotherm provides for a 60% improvement over the original FF isotherm. In general, the FF rescaling methodology is clearly observed to provide a significant improvement over using a generic FF like UFF/TraPPE.

4. Conclusions and future work

In this work, we first illustrated the use of the numerical disparity metric to evaluate the agreement of the various literature FF isotherms to experimental isotherms. GCMC simulations were used to investigate the adsorption characteristics of ethane and ethene in ZIF-8. We particularly focused on the low pressure regime (0.001 to 1.0 bar) where the host-guest interactions are dominant. Despite a significant quantitative disagreement with experimental

Table 9: Uptake disparities with respect to experimental results across different literature force fields between 0.001 to 1 bar.

Guest molecules	**Host/guest FF**	$U^{disp}(\%)$
Propane	ZhouFF/TraPPE	8
	GenericMOFs/TraPPE	9
	Rescaled UFF/TraPPE	12
	Dreiding/TraPPE	23
	AMBER/TraPPE	33
	UFF/TraPPE	72
Propene	ZhouFF/TraPPE	5
	GenericMOFs/TraPPE	5
	Rescaled UFF/TraPPE	21
	Dreiding/TraPPE	23
	AMBER/TraPPE	32
	UFF/TraPPE	84

isotherms, the LJ-based literature FFs correctly match the qualitative trend of ethane/ethene uptake. In spite of the seemingly good quantitative agreement with experimental isotherms, the Buckingham-based FFs fail to capture the qualitative trend in ethane/ethene uptake. Comparing among the LJ-based FFs, the system-specific FFs provided better quantitative agreement with experimental isotherms and Henry coefficients as compared to the generic class FFs. However, even the best system-specific FF in GenericMOFs/TraPPE overestimated ethane and ethene uptake by 29% with respect to experimental isotherms.

Furthermore, we have proposed two novel methodologies; a benchmarking methodology to evaluate the performance of any given FF in describing adsorption in the low pressure regime and a refinement procedure to rescale the parameters of any given force field to better describe the host-guest interactions and provide for simulation isotherms with close correlation to experimental isotherms at low pressure regimes. Both methodologies were developed based on a Henry coefficient reference, $K_H^{IS\_ref}$, generated using the importance sampling technique[29] at a fraction (1%) of the computational cost of a full *ab initio* Widom insertion simulation of 10^6 steps. The initial step in the importance sampling technique uses FFs to generate configurations for Widom insertion simulations but the resulting importance sam-

pled Henry coefficient, K_H^{IS}, and adsorption enthalpies, ΔH^{IS} was shown to be independent of the initial choice of FF. $K_H^{IS\_ref}$ was shown to match the experimental results with only 1.7% and 5.6% error for ethane and ethene respectively at 303K. Thus, $K_H^{IS\_ref}$ satisfies all the requirements to be a reliable reference i.e. (1) the reference results should be invariant of FFs (2) the methodology to obtain the reference needs to be independent of experimental input but the reference results themselves are required to have a close agreement with experimental input when those are available (3) the reference results need to be obtained with minimal computational overhead.

Using $K_H^{IS\_ref}$, we could then proceed with the two novel methodologies which is the subject of this work. For the first methodology involving the benchmarking of FFs, the initial step was to compute the Henry coefficients of the literature FFs, K_H^{FF}, using the Widom insertion method. Subsequently, K_H^{FF} was compared against $K_H^{IS\_ref}$. The literature FFs was ranked based on the disparity, K_H^{disp}, between these Henry coefficients. The predictive capability of this benchmarking methodology was validated against the uptake disparities of the simulation and experimental isotherms, U^{disp}, in the low pressure regime between 0.001 and 1 bar. The benchmarking methodology resulted in similar FF rankings to what was obtained with comparing the U^{disp}.

For the second methodology involving the rescaling of FF parameters, the ϵ_i parameter of FFs was modified such that its K_H^{FF} matches $K_H^{IS\_ref}$. To validate this methodology, five different FFs between UFF, Dreiding, AMBER, GenericMOFs and ZhouFF were rescaled separately for ethane and ethene. GCMC simulations were performed with these rescaled FFs, as such displaying a improvement over the original versions in literature. The best performing FF for ethane went from having a disparity of -16% to +9% and for ethene from 28% to 20%.

We further investigated the transferability of the FF rescaling methodology across higher pressure regimes i.e 0.1 to 8.1 bar for the ZIF-8/ethane and ethene systems and across larger guest molecules i.e propane and propene for the lower pressure regime. The rescaled

FF had good agreement with the experimental isotherm across the medium and higher pressure regimes with only -13% and -9% uptake disparity respectively for ZIF-8/ethane and ethene. The rescaled FF had good agreement with the experimental isotherm across the lower pressure regime between 0.001 to 1 bar with a 12% and 21% uptake disparity respectively for ZIF-8/propane and propene. Although the rescaled FFs could not outperform the system-specific FFs in terms of uptake disparity, the rescaled FFs outperformed the generic FFs significantly and posted a significant improvement of over 60% across both propane and propene over the original UFF/TraPPE FF.

The results of the transferability analysis support the notion that the two novel methodologies i.e. benchmarking and FF rescaling proposed in this work could be applied for a wider range of MOF systems and adsorbate guest molecules and also across higher pressure regimes. These methodologies are likely to be suited for alcohol molecules like propanol or butanol in MOFs where experimental results are lacking and FF based GCMC simulations are computationally intensive due to the large number of GCMC cycles required to achieve convergence in results. This makes it difficult to compare the isotherms of multiple FFs, hence, making it challenging to identify the best model for the system. In these cases, the use of the benchmarking and rescaling methodologies would help determine the best performing literature FF and also produce a FF that can adequately capture the adsorption properties at the low loading regime.

With regards to future work, the methodologies proposed in this work would be particularly applicable in the context of high-throughput screening where FFs are currently preferred over MLPs due to the former's superior computational efficiency. By rescaling existing generic FFs based on $K_H^{IS\_ref}$ from the importance sampling technique, the host-guest interactions can be described more accurately in a high throughput study. While MLPs can be trained to develop accurate adsorption isotherms for individual systems, training a generic MLP for a large high-throughput study is still unfeasible as this would still require a few thousand *ab initio* calculations for every individual system. Although, the methodolo-

gies proposed in this work also require *ab initio* calculations for individual systems to obtain $K_H^{IS\text{-}ref}$, the number of calculations required would be lower than what would be required to train a MLP as evidenced by the fraction of computational cost required for importance sampling as compared to that of an *ab initio* Widom insertion simulation. An improvement in the description of host-guest interactions with the use of rescaled FFs would be a significant boost for evaluating the performance of a large combination of adsorbent/adsorbate systems far more accurately than current methods. Further, the implications of the assumption of a rigid framework is something that can also certainly be further looked at in future work. Such work will most probably involve the training of a dedicated MLP, to describe the interaction energy of a guest molecule with a flexible host material, as well as advanced sampling schemes, such as Transition Matrix Monte Carlo, to account for the host flexibility in computing the lambda correction factor.

Acknowledgement

The authors acknowledge the financial support from the Research Board of Ghent University (BOF), the Flemish Government and Flanders Innovation and Entrepreneurship (VLAIO) through the Moonshot project MOONRISE under the grant number: HBC.2020.2612, the computational resources (Stevin Supercomputer Infrastructure) and services provided by the VSC (Flemish Supercomputer Center) funded by Ghent University, FWO and the Flemish Government, department EWI.

Supporting Information Available

Terminology abbreviations, details about the force fields, GCMC simulations and *ab initio* level of theory and convergence criteria tests performed in this work are provided in the Supporting Information. The relevant input files and simulation data, including the adsorption information format (AIF) files for the various adsorption isotherms presented in this work are available at https://doi.org/10.5281/zenodo.10709123.

References

(1) Sholl, D. S.; Lively, R. P. Seven chemical separations to change the world. *Nature* **2016**, *532*, 435–437.

(2) Yang, R. T. *Gas separation by adsorption processes*; World Scientific, 1997; Vol. 1.

(3) Do, D. D. *Adsorption analysis: Equilibria and kinetics (with cd containing computer MATLAB programs)*; World Scientific, 1998; Vol. 2.

(4) Yong, W. F.; Zhang, H. Recent advances in polymer blend membranes for gas separation and pervaporation. *Progress in Materials Science* **2021**, *116*, 100713.

(5) Baker, R. W. *Membrane technology and applications*; John Wiley & Sons, 2012.

(6) Luis, P. *Fundamental Modeling of Membrane Systems: Membrane and Process Performance*; Elsevier, 2018.

(7) Li, B.; Wen, H.-M.; Zhou, W.; Chen, B. Porous metal–organic frameworks for gas storage and separation: what, how, and why? *The journal of physical chemistry letters* **2014**, *5*, 3468–3479.

(8) Taylor, M. K.; Runčevski, T.; Oktawiec, J.; Gonzalez, M. I.; Siegelman, R. L.; Mason, J. A.; Ye, J.; Brown, C. M.; Long, J. R. Tuning the adsorption-induced phase change in the flexible metal–organic framework Co (bdp). *Journal of the American Chemical Society* **2016**, *138*, 15019–15026.

(9) Wang, K.; Feng, D.; Liu, T.-F.; Su, J.; Yuan, S.; Chen, Y.-P.; Bosch, M.; Zou, X.; Zhou, H.-C. A series of highly stable mesoporous metalloporphyrin Fe-MOFs. *Journal of the American Chemical Society* **2014**, *136*, 13983–13986.

(10) Jiang, J.; Furukawa, H.; Zhang, Y.-B.; Yaghi, O. M. High methane storage working capacity in metal–organic frameworks with acrylate links. *Journal of the American Chemical Society* **2016**, *138*, 10244–10251.

(11) Lee, D. T.; Corkery, P.; Park, S.; Jeong, H.-K.; Tsapatsis, M. Zeolitic imidazolate framework membranes: novel synthesis methods and progress toward industrial use. *Annual Review of Chemical and Biomolecular Engineering* **2022**, *13*, 529–555.

(12) Li, L.; Duan, Y.; Liao, S.; Ke, Q.; Qiao, Z.; Wei, Y. Adsorption and separation of propane/propylene on various ZIF-8 polymorphs: Insights from GCMC simulations and the ideal adsorbed solution theory (IAST). *Chemical Engineering Journal* **2020**, *386*, 123945.

(13) Chen, Y.; Qiao, Z.; Wu, H.; Lv, D.; Shi, R.; Xia, Q.; Zhou, J.; Li, Z. An ethane-trapping MOF PCN-250 for highly selective adsorption of ethane over ethylene. *Chemical Engineering Science* **2018**, *175*, 110–117.

(14) Dubbeldam, D.; Snurr, R. Recent developments in the molecular modeling of diffusion in nanoporous materials. *Molecular Simulation* **2007**, *33*, 305–325.

(15) Bendt, S.; Hovestadt, M.; Böhme, U.; Paula, C.; Döpken, M.; Hartmann, M.; Keil, F. J. Olefin/Paraffin Separation Potential of ZIF-9 and ZIF-71: A Combined Experimental and Theoretical Study. *European Journal of Inorganic Chemistry* **2016**, *2016*, 4440–4449.

(16) Qiao, Z.; Xu, Q.; Jiang, J. Computational screening of hydrophobic metal–organic frameworks for the separation of H 2 S and CO 2 from natural gas. *Journal of Materials Chemistry A* **2018**, *6*, 18898–18905.

(17) Krokidas, P.; Castier, M.; Economou, I. G. Computational study of ZIF-8 and ZIF-67 performance for separation of gas mixtures. *The Journal of Physical Chemistry C* **2017**, *121*, 17999–18011.

(18) Potoff, J. J.; Siepmann, J. I. Vapor–liquid equilibria of mixtures containing alkanes, carbon dioxide, and nitrogen. *AIChE journal* **2001**, *47*, 1676–1682.

(19) Lennox, M. J.; Bound, M.; Henley, A.; Besley, E. The right isotherms for the right reasons? Validation of generic force fields for prediction of methane adsorption in metal-organic frameworks. *Molecular Simulation* **2017**, *43*, 828–837.

(20) Gomez-Gualdron, D. A.; Gutov, O. V.; Krungleviciute, V.; Borah, B.; Mondloch, J. E.; Hupp, J. T.; Yildirim, T.; Farha, O. K.; Snurr, R. Q. Computational design of metal–organic frameworks based on stable zirconium building units for storage and delivery of methane. *Chemistry of Materials* **2014**, *26*, 5632–5639.

(21) Ozturk, T. N.; Keskin, S. Computational screening of porous coordination networks for adsorption and membrane-based gas separations. *The Journal of Physical Chemistry C* **2014**, *118*, 13988–13997.

(22) Wang, S. Comparative molecular simulation study of methane adsorption in metal-organic frameworks. *Energy & fuels* **2007**, *21*, 953–956.

(23) Vandenbrande, S.; Verstraelen, T.; Gutiérrez-Sevillano, J. J.; Waroquier, M.; Van Speybroeck, V. Methane adsorption in Zr-based MOFs: Comparison and critical evaluation of force fields. *The Journal of Physical Chemistry C* **2017**, *121*, 25309–25322.

(24) Glover, J.; Besley, E. Pore-filling contamination in metal–organic frameworks. *Physical Chemistry Chemical Physics* **2018**, *20*, 23616–23624.

(25) Cychosz Struckhoff, K.; Thommes, M.; Sarkisov, L. On the universality of capillary condensation and adsorption hysteresis phenomena in ordered and crystalline mesoporous materials. *Advanced Materials Interfaces* **2020**, *7*, 2000184.

(26) Fairen-Jimenez, D.; Galvelis, R.; Torrisi, A.; Gellan, A. D.; Wharmby, M. T.; Wright, P. A.; Mellot-Draznieks, C.; Dueren, T. Flexibility and swing effect on the adsorption of energy-related gases on ZIF-8: combined experimental and simulation study. *Dalton Transactions* **2012**, *41*, 10752–10762.

(27) Pérez-Pellitero, J.; Amrouche, H.; Siperstein, F. R.; Pirngruber, G.; Nieto-Draghi, C.; Chaplais, G.; Simon-Masseron, A.; Bazer-Bachi, D.; Peralta, D.; Bats, N. Adsorption of CO2, CH4, and N2 on zeolitic imidazolate frameworks: experiments and simulations. *Chemistry–A European Journal* **2010**, *16*, 1560–1571.

(28) Zhang, L.; Hu, Z.; Jiang, J. Sorption-induced structural transition of zeolitic imidazolate framework-8: A hybrid molecular simulation study. *Journal of the American Chemical Society* **2013**, *135*, 3722–3728.

(29) Vandenbrande, S.; Waroquier, M.; Van Speybroeck, V.; Verstraelen, T. Ab initio evaluation of Henry coefficients using importance sampling. *Journal of chemical theory and computation* **2018**, *14*, 6359–6369.

(30) Valenzano, L.; Civalleri, B.; Chavan, S.; Palomino, G. T.; Areán, C. O.; Bordiga, S. Computational and Experimental Studies on the Adsorption of CO, N2, and CO2 on Mg-MOF-74. *The Journal of Physical Chemistry C* **2010**, *114*, 11185–11191.

(31) Kundu, A.; Piccini, G.; Sillar, K.; Sauer, J. Ab Initio prediction of adsorption isotherms for small molecules in metal–organic frameworks. *Journal of the American Chemical Society* **2016**, *138*, 14047–14056.

(32) Alonso, G.; Bahamon, D.; Keshavarz, F.; Giménez, X.; Gamallo, P.; Sayós, R. Density functional theory-based adsorption isotherms for pure and flue gas mixtures on Mg-MOF-74. Application in CO2 capture swing adsorption processes. *The Journal of Physical Chemistry C* **2018**, *122*, 3945–3957.

(33) Lee, Y.; Poloni, R.; Kim, J. Probing gas adsorption in MOFs using an efficient ab initio widom insertion Monte Carlo method. *Journal of Computational Chemistry* **2016**, *37*, 2808–2815.

(34) C. Peirs, J.; De Proft, F.; Baron, G.; Van Alsenoy, C.; Geerlings, P. Non-empirical quan-

tum chemical calculation of Henry and separation constants and heats of adsorption for diatomic gases in faujasite. *Chem. Commun.* **1997**, 531–532.

(35) Goeminne, R.; Vanduyfhuys, L.; Van Speybroeck, V.; Verstraelen, T. DFT-Quality adsorption simulations in metal–organic frameworks enabled by machine learning Potentials. *Journal of Chemical Theory and Computation* **2023**, *19*, 6313–6325.

(36) De Vos, J. S.; Ravichandran, S.; Borgmans, S.; Vanduyfhuys, L.; Van Der Voort, P.; Rogge, S. M.; Van Speybroeck, V. High-Throughput Screening of Covalent Organic Frameworks for Carbon Capture Using Machine Learning. *Chemistry of Materials* **2024**, *36*, 4315–4330.

(37) Park, K. S.; Ni, Z.; Côté, A. P.; Choi, J. Y.; Huang, R.; Uribe-Romo, F. J.; Chae, H. K.; O'Keeffe, M.; Yaghi, O. M. Exceptional chemical and thermal stability of zeolitic imidazolate frameworks. *Proceedings of the National Academy of Sciences* **2006**, *103*, 10186–10191.

(38) Banerjee, R.; Phan, A.; Wang, B.; Knobler, C.; Furukawa, H.; O'Keeffe, M.; Yaghi, O. M. High-throughput synthesis of zeolitic imidazolate frameworks and application to CO2 capture. *Science* **2008**, *319*, 939–943.

(39) Sze Lai, L.; Fong Yeong, Y.; Keong Lau, K.; Shariff Az, M. Zeolite imidazole frameworks membranes for CO2/CH4 separation from natural gas: A review. *Journal of Applied Sciences* **2014**, *14*, 1161–1167.

(40) Awadallah-F, A.; Hillman, F.; Al-Muhtaseb, S. A.; Jeong, H.-K. On the nanogate-opening pressures of copper-doped zeolitic imidazolate framework ZIF-8 for the adsorption of propane, propylene, isobutane, and n-butane. *Journal of materials science* **2019**, *54*, 5513–5527.

(41) Huang, X.-C.; Lin, Y.-Y.; Zhang, J.-P.; Chen, X.-M. Ligand-directed strategy for

zeolite-type metal–organic frameworks: zinc (II) imidazolates with unusual zeolitic topologies. *Angewandte Chemie International Edition* **2006**, *45*, 1557–1559.

(42) Wu, Y.; Chen, H.; Liu, D.; Qian, Y.; Xi, H. Adsorption and separation of ethane/ethylene on ZIFs with various topologies: Combining GCMC simulation with the ideal adsorbed solution theory (IAST). *Chemical Engineering Science* **2015**, *124*, 144–153.

(43) Ke, Q.; Duan, Y.; Ji, Y.; Zhao, D.; Zhang, H.; Duan, C.; Li, L.; Wei, Y. Identical composition and distinct performance: how ZIF-8 polymorphs' structures affect the adsorption/separation of ethane and ethene. *Journal of Chemical & Engineering Data* **2021**, *66*, 3483–3492.

(44) Böhme, U.; Barth, B.; Paula, C.; Kuhnt, A.; Schwieger, W.; Mundstock, A.; Caro, J.; Hartmann, M. Ethene/ethane and propene/propane separation via the olefin and paraffin selective metal–organic framework adsorbents CPO-27 and ZIF-8. *Langmuir* **2013**, *29*, 8592–8600.

(45) Rappé, A. K.; Casewit, C. J.; Colwell, K.; Goddard III, W. A.; Skiff, W. M. UFF, a full periodic table force field for molecular mechanics and molecular dynamics simulations. *Journal of the American chemical society* **1992**, *114*, 10024–10035.

(46) Mayo, S. L.; Olafson, B. D.; Goddard, W. A. DREIDING: a generic force field for molecular simulations. *Journal of Physical chemistry* **1990**, *94*, 8897–8909.

(47) Duan, Y.; Wu, C.; Chowdhury, S.; Lee, M. C.; Xiong, G.; Zhang, W.; Yang, R.; Cieplak, P.; Luo, R.; Lee, T.; others A point-charge force field for molecular mechanics simulations of proteins based on condensed-phase quantum mechanical calculations. *Journal of computational chemistry* **2003**, *24*, 1999–2012.

(48) Dubbeldam, D.; Calero, S.; Ellis, D. E.; Snurr, R. Q. RASPA: molecular simulation

software for adsorption and diffusion in flexible nanoporous materials. *Molecular Simulation* **2016**, *42*, 81–101.

(49) Zhou, M.; Wang, Q.; Zhang, L.; Liu, Y.-C.; Kang, Y. Adsorption sites of hydrogen in zeolitic imidazolate frameworks. *The Journal of Physical Chemistry B* **2009**, *113*, 11049–11053.

(50) Jorgensen, W. L.; Maxwell, D. S.; Tirado-Rives, J. Development and testing of the OPLS all-atom force field on conformational energetics and properties of organic liquids. *Journal of the American Chemical Society* **1996**, *118*, 11225–11236.

(51) Bureekaew, S.; Amirjalayer, S.; Tafipolsky, M.; Spickermann, C.; Roy, T. K.; Schmid, R. MOF-FF–A flexible first-principles derived force field for metal-organic frameworks. *physica status solidi (b)* **2013**, *250*, 1128–1141.

(52) Allinger, N. L.; Yuh, Y. H.; Lii, J. H. Molecular mechanics. The MM3 force field for hydrocarbons. 1. *Journal of the American Chemical Society* **1989**, *111*, 8551–8566.

(53) Hertäg, L.; Bux, H.; Caro, J.; Chmelik, C.; Remsungnen, T.; Knauth, M.; Fritzsche, S. Diffusion of CH4 and H2 in ZIF-8. *Journal of Membrane Science* **2011**, *377*, 36–41.

(54) Widom, B. Some topics in the theory of fluids. *The Journal of Chemical Physics* **1963**, *39*, 2808–2812.

(55) Verstraelen, T.; Vanduyfhuys, L.; Vandenbrande, S.; Rogge, S. Yaff, yet another force field. `http://molmod.ugent.be/software/`, 2022.

(56) Perdew, J. P.; Burke, K.; Ernzerhof, M. Generalized gradient approximation made simple. *Physical review letters* **1996**, *77*, 3865.

(57) Grimme, S.; Ehrlich, S.; Goerigk, L. Effect of the damping function in dispersion corrected density functional theory. *Journal of computational chemistry* **2011**, *32*, 1456–1465.

(58) Tkatchenko, A.; DiStasio Jr, R. A.; Car, R.; Scheffler, M. Accurate and efficient method for many-body van der Waals interactions. *Physical review letters* **2012**, *108*, 236402.

(59) Bučko, T.; Lebègue, S.; Gould, T.; Ángyán, J. G. Many-body dispersion corrections for periodic systems: an efficient reciprocal space implementation. *Journal of Physics: Condensed Matter* **2016**, *28*, 045201.

(60) Blood-Forsythe, M. A.; Markovich, T.; DiStasio, R. A.; Car, R.; Aspuru-Guzik, A. Analytical nuclear gradients for the range-separated many-body dispersion model of noncovalent interactions. *Chemical science* **2016**, *7*, 1712–1728.

(61) Ambrosetti, A.; Reilly, A. M.; DiStasio, R. A.; Tkatchenko, A. Long-range correlation energy calculated from coupled atomic response functions. *The Journal of chemical physics* **2014**, *140*.

(62) Tkatchenko, A.; Ambrosetti, A.; DiStasio, R. A. Interatomic methods for the dispersion energy derived from the adiabatic connection fluctuation-dissipation theorem. *The Journal of Chemical Physics* **2013**, *138*.

(63) Kresse, G.; Furthmüller, J. Efficiency of ab-initio total energy calculations for metals and semiconductors using a plane-wave basis set. *Computational materials science* **1996**, *6*, 15–50.

(64) Kresse, G.; Furthmüller, J. Efficient iterative schemes for ab initio total-energy calculations using a plane-wave basis set. *Physical review B* **1996**, *54*, 11169.

(65) Blöchl, P. E. Projector augmented-wave method. *Physical review B* **1994**, *50*, 17953.

(66) Fischer, M.; Bell, R. G. Interaction of hydrogen and carbon dioxide with sod-type zeolitic imidazolate frameworks: a periodic DFT-D study. *CrystEngComm* **2014**, *16*, 1934–1949.

(67) Han, B.; Chakraborty, A.; Saha, B. B. Isosteric Heats and Entropy of Adsorption in Henry's Law Region for Carbon and MOFs Structures for Energy Conversion Applications. *International Journal of Heat and Mass Transfer* **2022**, *182*, 122000.

(68) Bux, H.; Chmelik, C.; Krishna, R.; Caro, J. Ethene/ethane separation by the MOF membrane ZIF-8: Molecular correlation of permeation, adsorption, diffusion. *Journal of membrane science* **2011**, *369*, 284–289.

Table of Contents Graphic